UDC 546(571+861+814+22)

Sharafat H. Mammadov, Asif N. Mammadov

STUDY OF VARIABLE COMPOSITION PHASE ALONG THE $AgSbS_2$–Ag_8SnS_6 SECTION IN THE Ag–Sn–Sb–S QUATERNARY SYSTEM

Institute of Catalysis and Inorganic Chemistry named after academician M.F. Nagiev, Baku, Republic of Azerbaijan

Ternary chalcogenide compounds, in particular phases based on silver and antimony sulfides, have attracted research attention because of their potential applications. Antimony chalcogenides are semiconductor materials with photosensitive properties and are therefore widely used in photoresistors, photocells, electron-beam devices, solar cells, semiconductor sensitizers, micromechanical, and optical devices. In the study of the Ag_8SnS_6–$AgSbS_2$ system, the initial compounds (Ag_8SnS_6, $AgSbS_2$) were first synthesized. Elements of at least 99.99 wt.% purity were used in the synthesis. Synthesis involving a volatile component (sulfur) was carried out using a visual-combined method. Alloys of the $AgSbS_2$–Ag_8SnS_6 system were synthesized from ligatures using the ampoule method in a vertical furnace. The maximum temperature of alloy synthesis was 1200 K. The synthesis lasted for 3.5 h with mechanical stirring and slow cooling. Annealing of the $AgSbS_2$–Ag_8SnS_6 alloys was carried out in evacuated, sealed quartz ampoules at 550–700 K for 380 h. The paper presents data on phase equilibria in the $AgSbS_2$–Ag_8SnS_6 system. Based on the results of X-ray structural and microstructural analyses, differential thermal analysis, and thermodynamic calculations, a phase diagram of the $AgSbS_2$–Ag_8SnS_6 section over a wide concentration range was constructed. It was found that this is a quasi-binary section of the ternary system Ag_2S–SnS_2–Sb_2S_3. The $AgSbS_2$–Ag_8SnS_6 system is eutectic; the eutectic point corresponds to 38 mol.% Ag_8SnS_6 and 750 K. The homogeneity regions based on $AgSbS_2$ and Ag_8SnS_6 were determined. Solid solutions based on $AgSbS_2$ are formed at room temperature (300 K) at 10 mol.% Ag_8SnS_6, whereas solid solutions based on Ag_8SnS_6 are formed at 16 mol.% $AgSbS_2$. Solid solutions based on $AgSbS_2$ crystallize in the monoclinic syngony, and those based on Ag_8SnS_6 crystallize in the rhombic syngony.

Keywords: eutectic, solid solution, Ag_2S–SnS_2–Sb_2S_3, phase diagram, system, Gibbs free energy.

DOI: 10.32434/0321-4095-2025-163-6-98-104

Introduction

Ternary chalcogenide compounds, in particular phases based on silver and antimony sulfides, have attracted the attention of researchers due to their potential applications. Antimony chalcogenides are semiconductor materials with photosensitive properties, and therefore these compounds are widely used in photoresistors, photocells, electron-beam devices, solar cells, semiconductor sensitizers, micromechanical and optical devices. The search for and acquisition of new

functionally promising materials, especially the growth of their high-purity single crystals, and the study of the temperature-composition dependence of the corresponding systems is of great importance from a technological point of view [1–5].

The $AgSbS_2$ compound occurs in nature as the mineral miargyrite. This compound was obtained in laboratory conditions during the study of the $Ag_2S–Sb_2S_3$ section [6]. According to [6], this section is quasi-binary and forms two congruently melting compounds Ag_3SbS_3 and $AgSbS_2$. $AgSbS_2$ crystallizes in the monoclinic syngony with the following parameters:[1] a=12.861 Å, b=4.409 Å, c=13.282 Å, β=98.21°. In study [7], $AgSbS_2$ was synthesized using microwave radiation. In study [4], the phase diagram of $Ag_2SnS_3–AgSbS_2$ was constructed, and the boundaries of solid solutions based on ternary compounds were determined.

Silver thiostannates (Ag_8SnX_6; X=S,Se) are promising inorganic materials with functional electrophysical properties. The literature contains information on the study of the side systems that make up the quasi-ternary system $Ag_2S–SnS_2–Sb_2S_3$. In a study of the $Ag_2S–SnS_2$ system [8], it was established that three compounds exist with the following compositions: Ag_8SnS_6, Ag_2SnS_3 and $Ag_2Sn_2S_5$. The Ag_8SnS_6 compound melts congruently at 1125 K and has two polymorphic forms. The transition from high-temperature modification to high-temperature modification occurs at a temperature of 444 K [9]. The low-temperature modification of Ag_8SnS_6 has a rhombic structure (space group $Pmn2_1$) with lattice parameters: a=15.298 Å, b=7.548 Å, c=10.699 Å [10]. The high-temperature modification of Ag_8SnS_6 exhibits a cubic structure (space group F-43m, a=10.850 Å) [11]. Kitazawa et al. [12] also studied the $Ag_2S–SnS_2$ systems. They determined that the compounds of the compositions $Ag_4Sn_3S_8$, Ag_8SnS_6 and Ag_2SnS_3 are formed in the systems.

There is no information on the phase diagram of $Ag_8SnS_6–AgSbS_2$ in the literature. The aim of this study is to investigate the phase diagram $Ag_8SnS_6–AgSbS_2$ of the four-component Ag–Sn–Sb–S system and determine the boundaries of solid solutions based on both components.

Experimental

When studying the $Ag_8SnS_6–AgSbS_2$ system, the initial compounds (Ag_8SnS_6 and $AgSbS_2$) were first synthesized. Elements of at least 99.99 wt.% purity were used in the synthesis. Synthesis involving a volatile component, in this case sulfur, was carried out using a visual-combined method. Alloys of the $AgSbS_2–Ag_8SnS_6$ system were synthesized from ligatures using the ampoule method in a vertical furnace. The maximum temperature of alloy synthesis was 1200 K. The synthesis lasted for 3.5 h using a mechanical stirrer with slow cooling. Annealing of the $AgSbS_2–Ag_8SnS_6$ system alloys was carried out in evacuated and sealed quartz ampoules at 550–700 K for 380 h. The annealed samples were quenched in cold water.

The interaction in the $Ag_8SnS_6–AgSbS_2$ systems was studied by differential thermal analysis (DTA), X-ray phase analysis (XPA), microstructural analysis (MSA), and density determination. XPA was performed on a D2 PHASER model X-ray device using CuKα radiation (Ni filter). DTA of the alloys of the system was carried out in evacuated quartz ampoules on a differential scanning calorimeter NETZSCH 404 F1 Pegasus system and using NETZSCH Proteus software. The accuracy of temperature measurements was ±2K.

When studying the microstructure of the alloys, an etchant of the composition NH_4NO_3 (3–8 wt.%)+$K_2Cr_2O_7$ (0.02–0.5 wt.%)+concentrated H_2SO_4 was used, the etching time was 20 s. The MSA of the alloys of the systems was studied using a metallographic microscope MIM-8 on pre-etched sections. The phase diagram of the $AgSbS_2–Ag_8SnS_6$ system was constructed using experimental methods of physicochemical analysis (DTA, MSA, X-ray fluorescence, microhardness and density measurements) with the use of thermodynamic calculations.

Results and discussion

Experimental results

To study the phase equilibrium in the $AgSbS_2–Ag_8SnS_6$ system, 12 alloys of different compositions were synthesized (Table 1).

Based on the results of physicochemical analysis (XRD, DTA, MSA and density determination), a T *vs.* composition phase diagram of the $AgSbS_2–Ag_8SnS_6$ system was constructed (Fig. 1). The DTA results showed that all thermograms of alloys of the system with a composition of 30–70 mol.% Ag_8SnS_6 have three endothermic effects except for those containing 38 mol.% Ag_8SnS_6, and four endothermic effects are observed for alloys of 90 and 80 mol.% $AgSbS_2$ (Table 1). The effects at 640 K correspond to the phase transition $\beta(AgSbS_2)\leftrightarrow\beta'(AgSbS_2)$.

As can be seen from Fig. 1, the phase diagram of the $AgSbS_2–Ag_8SnS_6$ system belongs to the eutectic type with limited solubility of the initial components in the solid state. At room temperature, the solubility of a system based on $AgSbS_2$ is 10 mol.% Ag_8SnS_6, while the solubility of a system based on Ag_8SnS_6 is

[1] Miargyrite AgSbS2. P. 2001-2005. Mineral Data Publishing, version 1. handbookof-mineralogy.org/pdfs/miargyrite.pdf.

16 mol.% $AgSbS_2$. At the eutectic temperature, the solubility reaches 15 and 25 mol.%, respectively. The eutectic has a composition of 38 mol.% Ag_8SnS_6 and crystallizes at a temperature of 750 K.

The study of the microstructure of samples of the $AgSbS_2$–Ag_8SnS_6 system showed that they are all two-phase, with the exception of alloys near the initial components (0–10 and 84–100 mol.% Ag_8SnS_6), which are solid solutions. The results of XRD and MSA of the alloys of the studied system are consistent with the DTA data and confirm the existence of solid solutions based on $AgSbS_2$ and Ag_8SnS_6. According to XRD data (Fig. 2), the diffraction lines of alloys containing 0–10 mol.% Ag_8SnS_6 are identical to the diffraction pattern of $AgSbS_2$. The diffraction lines of alloys with compositions of 10–84 mol.% Ag_8SnS_6 consist of a set of reflection lines of $AgSbS_2$ and Ag_8SnS_6 phases. The diffraction patterns of alloys from the region of solid solutions of 84–100 mol.% Ag_8SnS_6 are identical to the diffraction pattern of Ag_8SnS_6. The above alloys have solid solution structures.

Table 1

Composition and DTA results of alloys of the $AgSbS_2$–Ag_8SnS_6 system

Composition, mol.% $AgSbS_2$	Thermal effects, K
100	785
90	640; 660; 765; 780
80	640; 645; 750; 775
70	650; 750; 765
62	750 (eutectic)
60	640; 750; 770
50	640; 750; 875
40	640; 750; 935
30	640; 750; 980
20	805; 1020
10	960; 080
0.0	1155

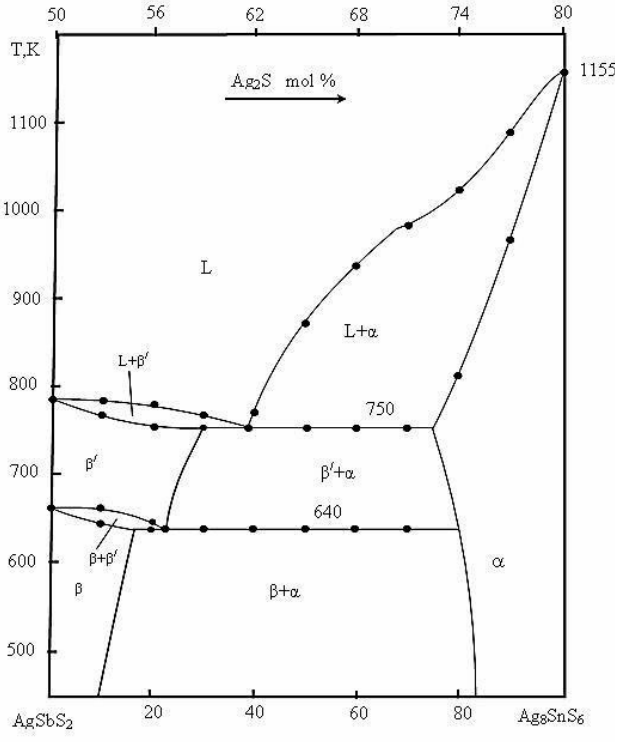

Fig. 1. Phase diagram of the $AgSbS_2$–Ag_8SnS_6 system

To determine the boundaries of solid solutions in the $AgSbS_2$–Ag_8SnS_6 system, alloys of different compositions on both sides were additionally synthesized. The resulting alloys were annealed at 700 and 550 K for 170 h and then quenched (Table 2).

Solid solutions based on $AgSbS_2$ crystallize in monoclinic syngony, while solid solutions based on thiostannates (Ag_8SnS_6) crystallize in orthorhombic syngony. As can be seen from Table 3, the orthorhombic lattice parameters increase with an increase in the $AgSbS_2$ content.

Measurement of the density of alloys in the $AgSbS_2$–Ag_8SnS_6 system showed that the density varies within the density range of $AgSbS_2$ and Ag_8SnS_6 (Table 4).

As can be seen from Table 4, the microhardness values of alloys rich in $AgSbS_2$ and Ag_8SnS_6 increase significantly from 1400 to 1570 MPa (β) and from 2710 to 2885 MPa (α), respectively, upon the formation of solid solutions.

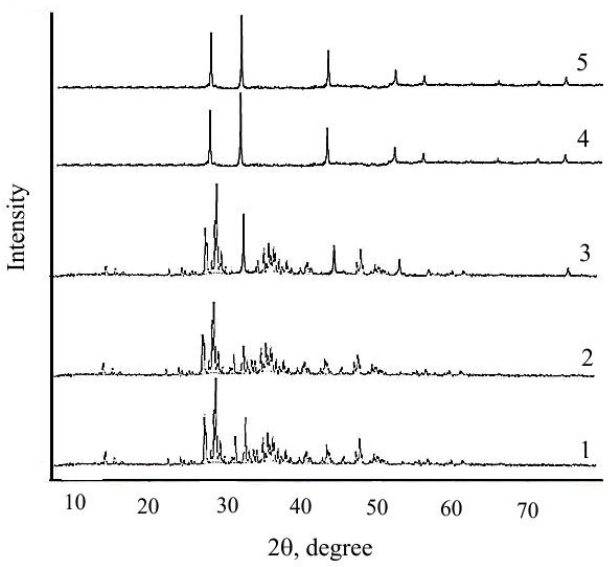

Fig. 2. XRD patterns of alloys of the $AgSbS_2$–Ag_8SnS_6 system: 1 – Ag_8SnS_6; 2 – 85 mol.% Ag_8SnS_6; 3 – 50 mol.% Ag_8SnS_6; 4 – 10 mol.% Ag_8SnS_6; 5 – $AgSbS_2$

Thermodynamic calculations

The boundaries of solid solutions based on α(Ag_8SnS_6) and β($AgSbS_2$) were refined using the temperature-concentration dependence of the Gibbs free energy. The Ag_8SnS_6 and $AgSbS_2$ compounds differ significantly in composition and crystallographic data. Therefore, for thermodynamic calculations, a modified version of the regular solution model was used, taking into account the dependence of the mixing parameter on the composition [4,13]:

$$\Delta G_T^{mix} = ax^m(1-x)^n + RT\left[x\ln x + (1-x)\ln(1-x)\right]. \quad (1)$$

Here the first term represents the enthalpy of mixing of solid solutions within the framework of the asymmetric version of the regular solution model (according to the model of strictly regular solutions m=1; n=1), the second term represents the configurational entropy of mixing of solid solutions. The dependences of free energy of mixing of the solid solutions of Ag_8SnS_6 and $AgSbS_2$ are visualized in Fig. 3, which allows clarifying the boundaries of solid solutions in the Ag_8SnS_6–$AgSbS_2$ system (Fig. 1). The analytical dependences of the Gibbs free energy of mixing on the composition for solid solutions based on the compounds Ag_8SnS_6 and $AgSbS_2$ are presented in the captions to Fig. 3. The calculations were performed using the OriginLab program.

Conclusions

1. The phase diagram of the $AgSbS_2$–Ag_8SnS_6 system was studied and constructed using physicochemical analysis methods (XRD, DTA, and MSA). It was found that the system is a quasi-binary section of the Ag_2S–SnS_2–Sb_2S_3 ternary system and belongs to the eutectic type.

2. The formation of solid solutions based on the initial components was detected in the $AgSbS_2$–Ag_8SnS_6 system. At room temperature, the solubility of a system based on $AgSbS_2$ is 10 mol.% Ag_8SnS_6, and the solubility of a system based on Ag_8SnS_6 is 16 mol.% $AgSbS_2$.

3. Within the framework of the asymmetric version of the regular solution model, the dependences of the Gibbs free energy on temperature and composition were determined, which made it possible to clarify the boundaries of solid solutions based on $AgSbS_2$ and Ag_8SnS_6 compounds.

Table 2

Annealing of alloys of the $AgSbS_2$–Ag_8SnS_6 system at temperatures of 550 and 700 K

Composition, mol.%		Phases		Composition, mol.%		Phases	
$AgSbS_2$	Ag_8SnS_6	550 K	700 K	$AgSbS_2$	Ag_8SnS_6	550 K	700 K
0.0	100	α	α	18	82	β+α	β+α
2.0	98	α	α	100	0,0	β	β
4.0	96	α	α	98	2.0	β	β
6.0	94	α	α	96	4.0	β	β
8.0	92	α	α	94	6.0	β	β
10	90	α	α	92	8.0	β	β
12	88	α	α	90	10	β+α	β
14	86	β+α	α	88	12	β+α	β+α
16	84	β+α	α				

Table 3

Crystal lattice parameters of solid solutions based on Ag_8SnS_6 in the $AgSbS_2$–Ag_8SnS_6 system

Composition, mol.% $AgSbS_2$	Lattice parameters, A^0	Pr.gr	Syngony
0.00	a=15.298; b=7.548; c=10.699	$Pmn2_1$	rhombic
0.02	a=15.301; b=7.550; c=10.700	$Pmn2_1$	rhombic
0.04	a=15.303; b=7.553; c=10.704	$Pmn2_1$	rhombic
0.06	a=15.304; b=7.555;c=10.705	$Pmn2_1$	rhombic
0.08	a=15.306; b=7.556; c=10.706	$Pmn2_1$	rhombic
0.10	a=15.308; b=7.561; c=10.707	$Pmn2_1$	rhombic
0.12	a=15.310; b=7.562; c=10.709	$Pmn2_1$	rhombic
0.14	a=15.313; b=7.569; c=10.714	$Pmn2_1$	rhombic

Table 4

Microhardness and density of alloys of the $AgSbS_2$–Ag_8SnS_6 system

Composition, mol.% $AgSbS_2$	Microhardness, MPa	Density, g/cm^3
100	1400	5.28
90	1570	5.37
80	1575	5.49
70	1560	5.54
62	1560	5.62
60	not measured	5.64
50	not measured	5.73
40	2885	5.84
30	2880	5.94
20	2880	6.05
10	2885	6.16
0	2710	6.28

REFERENCES

1. *Mammadov F.M.* New version of the phase diagram of the MnTe-Ga_2Te_3 system // New Materials, Compounds and Applications. – 2021. – Vol.5. – No. 2. – P.116-121.

2. *Mammadov Sh.H.* The study of the quasi-triple system FeS-Ga_2S_3-Ag_2S by a $FeGa_2S_4$-$AgGaS_2$ section // Kondensirovannye Sredy Mezhfaznye Granitsy. – 2020. – Vol.22. – No. 2. – P.232-237.

3. *Mammadov S.H., Gurbanov G.R., Ismailova R.A.* Phase diagram of the $AgGaS_2$–$PbGa_2S_4$ system // Voprosy Khimii i Khimicheskoi Tekhnologii. – 2025. – No. 1. – P.22-26.

4. *Mammadov S.H., Mammadov A.N., Kurbanova R.C.* Quasi-binary section Ag_2SnS_3–$AgSbS_2$ // Russ. J. Inorg. Chem. – 2020. – Vol.65. – No. 2. – P.217-221.

5. *Mammadov F.M.* FeS-$FeGa_2S_4$-$FeGaInS_4$ system // Chem. Probl. – 2020. – Vol.18. – No. 2. – P.214-221.

6. *Keighin C.W., Noneva R.M.* The system Ag-Sb-S from 600°C to 200°C // Mineral. Deposita. – 1969. – Vol.4. – P.153-171.

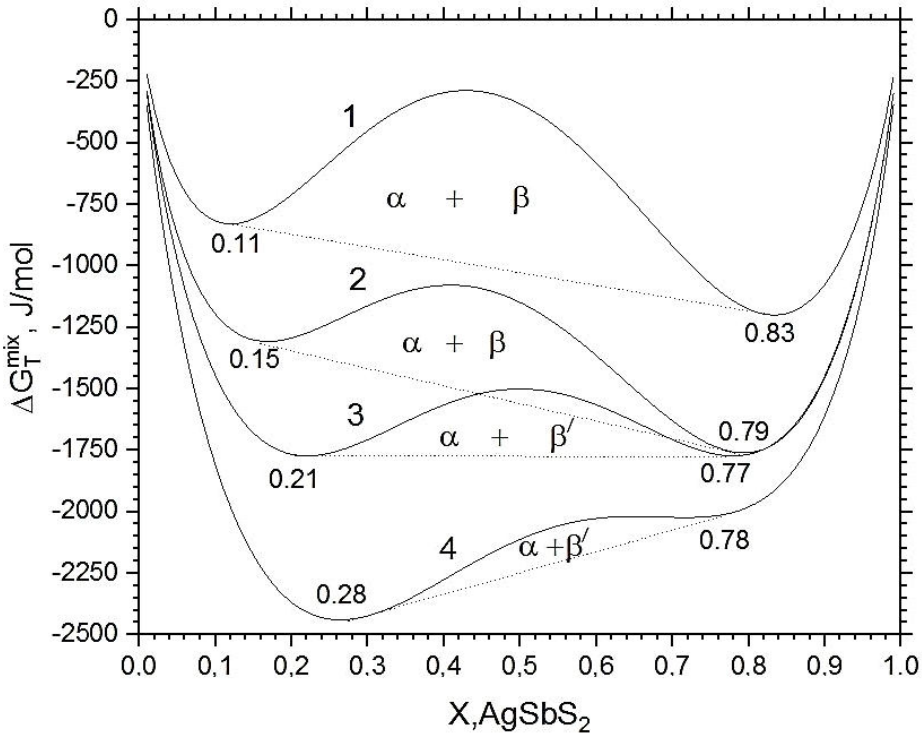

Fig. 3. Dependences of the free energy of formation of solid solutions in the Ag_8SnS_6 and $AgSbS_2$ system (x is the mole fraction of $AgSbS_2$) on the temperature and composition:

1 – $\Delta G_T^{mix} = 33000\cdot(1-x)^2x^{1.7} + 8.314\cdot500\cdot x\ln x + 8.314\cdot500\cdot(1-x)\ln(1-x)$;

2 – $\Delta G_T^{mix} = 33000\cdot(1-x)^2x^{1.7} + 8.314\cdot640\cdot x\ln x + 8.314\cdot640\cdot(1-x)\ln(1-x)$;

3 – $\Delta G_T^{mix} = 35000\cdot(1-x)^2x^{2} + 8.314\cdot640\cdot x\ln x + 8.314\cdot640\cdot(1-x)\ln(1-x)$;

4 – $\Delta G_T^{mix} = 33000\cdot(1-x)^{1.8}x^{2.1} + 8.314\cdot750\cdot x\ln x + 8.314\cdot750\cdot(1-x)\ln(1-x)$

7. *Tipcompor N., Thongtem S., Thongtem T.* Characterization of cubic $AgSbS_2$ nanostructured flowers synthesized by microwave-assisted refluxing method // J. Nanomater. – 2013. – Vol.2013. – Art. No. 970489.

8. *Kokhan O.P.* The interactions in Ag_2X-$B^{IV}X_2$ (BIV – Si, Ge, Sn; X – S, Se) systems and the properties of compounds. – Doctoral thesis. – Uzhgorod, 1996.

9. *Wang N., Fan A.K.* An experimental study of the Ag_2S–SnS_2 pseudobinary join // Neues Jahrb. Mineral. Abh. – 1989. – Vol.160. – P.33-36.

10. *Wang N.* New data for Ag_8SnS_6 (canfeildite) and Ag_8GeS_6 (argyrodite) // Neues Jahrb. Mineral. Monatsh. – 1978. – P.269-272.

11. *Gorochov O.* Les composes Ag_8MX_6 (M = Si, Ge, Sn et X=S, Se, Te) // Bull. Soc. Chim. Fr. – 1968. – No. 6. – P.2263-2275.

12. *Kitazawa H., Kitakeze A., Sugaki A.* Phase relation on the Ag–Sn–S system // Collect. Abstr. Mineral. Soc. Jap. – 1985. – No. 19.

13. *Determination* of the boundaries of solid solutions in the MnTe-Sb_2Te_3 and SnTe-Sb_2Te_3 systems / Orujlu E.N., Seidzade A.E., Mammadov A.N., Tagiev D.B., Babanly M.B. // Abstr. of the 11th International Conference on Theory and Application of Soft Computing, Computing with Words and Perceptions and Artificial Intelligence. – ICSCCW-2021. – Lecture Notes in Networks and Systems. – 2022. – Vol.362. – P.513-521.

Received 02.05.2025

ДОСЛІДЖЕННЯ ФАЗИ ЗМІННОГО СКЛАДУ УЗДОВЖ ПЕРЕТИНУ $AgSbS_2$–Ag_8SnS_6 У ЧЕТВЕРТНІЙ СИСТЕМІ Ag–Sn–Sb–S

Шарафат Х. Маммадов, Асиф Н. Маммадов

Трикомпонентні халькогенідні сполуки, зокрема фази на основі сульфідів срібла та сурми, викликали інтерес у дослідників через їхні потенційні застосування. Сурмові халькогеніди є напівпровідниковими матеріалами з фоточутливими властивостями, тому ці сполуки широко застосовуються у фоторезисторах, фотоелементах, електронно-променевих приладах, сонячних елементах, напівпровідникових сенситизаторах, мікромеханічних та оптичних пристроях. При вивченні системи Ag_8SnS_6–$AgSbS_2$ спочатку було синтезовано вихідні сполуки (Ag_8SnS_6, $AgSbS_2$). Для синтезу використовували елементи чистотою не менше 99,99 мас.%. Синтез із використанням леткого компоненту (сірки) проводили візуально-комбінованим методом. Сплави системи Ag_8SnS_6–$AgSbS_2$ отримували із лігатур ампульним методом у вертикальній печі. Максимальна температура синтезу сплавів становила 1200 K. Синтез тривав 3,5 год з механічним перемішуванням і повільним охолодженням. Відпал сплавів системи Ag_8SnS_6–$AgSbS_2$ проводили у вакуумованих і запаяних кварцових ампулах при 550–700 K протягом 380 год. У роботі наведено дані щодо фазової рівноваги в системі $AgSbS_2$–Ag_8SnS_6. На основі результатів рентгеноструктурного та мікроструктурного аналізів, диференційного термічного аналізу та термодинамічних розрахунків було побудовано фазову діаграму перетину $AgSbS_2$–Ag_8SnS_6 у широкому концентраційному діапазоні. Встановлено, що це квазібінарний переріз трикомпонентної системи Ag_2S–SnS_2–Sb_2S_3. Система $AgSbS_2$–Ag_8SnS_6 є евтектичною; координати евтектики відповідають 38 мол.% Ag_8SnS_6 та 750 K. У системі визначено ділянки гомогенності, що базуються на $AgSbS_2$ та Ag_8SnS_6. При кімнатній температурі (300 K) тверді розчини на основі $AgSbS_2$ утворюються при 10 мол.% Ag_8SnS_6, тоді як тверді розчини на основі Ag_8SnS_6 утворюються до 16 мол.% $AgSbS_2$. Тверді розчини на основі $AgSbS_2$ кристалізуються в моноклінній сингонії, а ті, що базуються на Ag_8SnS_6, – у ромбічній сингонії.

Ключові слова: евтектика; твердий розчин; Ag_2S–SnS_2–Sb_2S_3; фазова діаграма; система; вільна енергія Гіббса.

STUDY OF VARIABLE COMPOSITION PHASE ALONG THE $AgSbS_2$–Ag_8SnS_6 SECTION IN THE Ag–Sn–Sb–S QUATERNARY SYSTEM

Sharafat H. Mammadov *, Asif N. Mammadov

Institute of Catalysis and Inorganic Chemistry named after academician M.F. Nagiev, Baku, Republic of Azerbaijan

* **e-mail: chemminfo@gmail.com**

Ternary chalcogenide compounds, in particular phases based on silver and antimony sulfides, have attracted research attention because of their potential applications. Antimony chalcogenides are semiconductor materials with photosensitive properties and are therefore widely used in photoresistors, photocells, electron-beam devices, solar cells, semiconductor sensitizers, micromechanical, and optical devices. In the study of the Ag_8SnS_6–$AgSbS_2$ system, the initial compounds (Ag_8SnS_6, $AgSbS_2$) were first synthesized. Elements of at least 99.99 wt.% purity were used in the synthesis. Synthesis involving a volatile component (sulfur) was carried out using a visual-combined method. Alloys of the $AgSbS_2$–Ag_8SnS_6 system were synthesized from ligatures using the ampoule method in a vertical furnace. The maximum temperature of alloy synthesis was 1200 K. The synthesis lasted for 3.5 h with mechanical stirring and slow cooling. Annealing of the $AgSbS_2$–Ag_8SnS_6 alloys was carried out in evacuated, sealed quartz ampoules at 550–700 K for 380 h. The paper presents data on phase equilibria in the $AgSbS_2$–Ag_8SnS_6 system. Based on the results of X-ray structural and microstructural analyses, differential thermal analysis, and thermodynamic calculations, a phase diagram of the $AgSbS_2$–Ag_8SnS_6 section over a wide concentration range was constructed. It was found that this is a quasi-binary section of the ternary system Ag_2S–SnS_2–Sb_2S_3. The $AgSbS_2$–Ag_8SnS_6 system is eutectic; the eutectic point corresponds to 38 mol.% Ag_8SnS_6 and 750 K. The homogeneity regions based on $AgSbS_2$ and Ag_8SnS_6 were determined. Solid solutions based on $AgSbS_2$ are formed at room temperature (300 K) at 10 mol.% Ag_8SnS_6, whereas solid solutions based on Ag_8SnS_6 are formed at 16 mol.% $AgSbS_2$. Solid solutions based on $AgSbS_2$ crystallize in the monoclinic syngony, and those based on Ag_8SnS_6 crystallize in the rhombic syngony.

Keywords: eutectic; solid solution; Ag_2S–SnS_2–Sb_2S_3; phase diagram; system; Gibbs free energy.

REFERENCES

1. Mammadov FM. New version of the phase diagram of the $MnTe$-Ga_2Te_3 system. *New Materials, Compounds and Applications*. 2021; 5(2): 116-121.

2. Mammadov Sh.H. The study of the quasi-triple system FeS-Ga_2S_3-Ag_2S by a $FeGa_2S_4$-$AgGaS_2$ section. *Kondensirovannye Sredy Mezhfaznye Granitsy*. 2020; 22(2): 232-237. doi: 10.17308/kcmf.2020.22/2835.

3. Mammadov SH, Gurbanov GR, Ismailova RA. Phase diagram of the $AgGaS_2$–$PbGa_2S_4$ system. *Voprosy Khimii i Khimicheskoi Tekhnologii*. 2025; (1): 22-26. doi: 10.32434/0321-4095-2025-158-1-22-26.

4. Mammadov SH, Mammadov AN, Kurbanova RC. Quasi-binary section Ag_2SnS_3–$AgSbS_2$. *Russ J Inorg Chem*. 2020; 65: 217-221. doi: 10.1134/S003602362001012X.

5. Mammadov FM. FeS-$FeGa_2S_4$-$FeGaInS_4$ system. *Chem Probl*. 2020; 18(2): 214-221. doi: 10.32737/2221-8688-2020-2-214-221.

6. Keighin CW, Noneva RM. The system Ag-Sb-S from 600°C to 200°C. *Mineral Deposita*. 1969; 4: 153-171. doi: 10.1007/BF00208050.

7. Tipcompor N, Thongtem S, Thongtem T. Characterization of cubic $AgSbS_2$ nanostructured flowers synthesized by microwave-assisted refluxing method. *J Nanomater*. 2013; 2013: 970489. doi: 10.1155/2013/970489.

8. Kokhan OP. *The interactions in Ag_2X–$BIVX_2$ (BIV – Si, Ge, Sn; X – S, Se) systems and the properties of compounds* [doctoral thesis]. Uzhgorod (Ukraine); 1996.

9. Wang N, Fan AK. An experimental study of the Ag_2S–SnS_2 pseudobinary join. *Neues Jahrbuch fur Mineralogie-Abhandlungen*. 1989; 160: 33-36.

10. Wang N. New data for Ag_8SnS_6 (canfeildite) and Ag_8GeS_6 (argyrodite). *Neues Jahrbuch fur Mineralogie-Monatshefte*. 1978; 269-272.

11. Gorochov O. Les composes Ag_8MX_6 (M = Si, Ge, Sn et X=S, Se, Te). *Bull Soc Chim Fr*. 1968; (6): 2263-2275.

12. Kitazawa H, Kitakeze A, Sugaki A. Phase relation on the Ag–Sn–S system. *Collect Abstr Mineral Soc Jap*. 1985; (19).

13. Orujlu EN, Seidzade AE, Mammadov AN, Tagiev DB, Babanly MB. Determination of the boundaries of solid solutions in the $MnTe$-Sb_2Te_3 and $SnTe$-Sb_2Te_3 systems. In: Aliev RA, Kacprzyk J, Pedrycz W, Jamshidi M, Babanli M, Sadikoglu FM, editors. *11th International Conference on Theory and Application of Soft Computing, Computing with Words and Perceptions and Artificial Intelligence - ICSCCW-2021*. Lecture Notes in Networks and Systems. Vol 362. Springer, Cham; 2022. p. 513-521. doi: 10.1007/978-3-030-92127-9_69.